Chinese Chemical Letters 36 (2025) 110398

Contents lists available at ScienceDirect

Chinese Chemical Letters

journal homepage: www.elsevier.com/locate/cclet

Reticulated lanthanum (La) carbonate-carbon composite for efficient phosphorus removal from eutrophic wastewater

Xiuxiu Jia[a,1], Tao Yin[a,1], Nianpeng Li[a], Hua Zhang[b], Anxian Shi[b], Abdukader Abdukayum[c], Sanshuang Gao[a], Guangzhi Hu[a,*]

[a] Institute for Ecological Research and Pollution Control of Plateau Lakes, School of Ecology and Environmental Science, Yunnan University, Kunming 650504, China
[b] Green Food Development Center of Zhaotong City, Zhaotong 657099, China
[c] Xinjiang Key Laboratory of Novel Functional Materials Chemistry, College of Chemistry and Environmental Sciences, Kashi University, Kashi 844000, China

ARTICLE INFO

Article history:
Received 8 May 2024
Revised 13 August 2024
Accepted 31 August 2024
Available online 1 September 2024

Keywords:
LACC
Phosphorus removal
Chemical adsorption
Fast absorption
Desorption

ABSTRACT

A porous lanthanum (La) carbonate-carbon composite (LaCC) was prepared by vacuum-freeze-drying and pyrolysis techniques to remove phosphorus (P) from wastewater. Using polyethylene glycol as a carbon skeleton template, and the organic ligands are removed during pyrolysis, resulting in the creation of many pore structures. The LaCC showed excellent P removal performance and selectivity over a wide pH range (3–10). It exhibited a rapid adsorption rate and could hold up to 119.5 mg P/g. Fixed-bed column experiments showed that under dynamic conditions, just 1 g of LaCC effectively treated 60 L of P-contaminated wastewater with an initial concentration of 2 mg/L, meeting the primary discharge standard of <0.5 mg/L according to the comprehensive sewage guidelines of China. Bacterial experiments showed that the LaCC could inhibit the growth of *Escherichia coli*, indicating that it has both P removal and bacterial inhibition effects, which can greatly improve the application range of adsorbents.

To prevent the eutrophication of water bodies, it is critical to carry out deep removal of phosphorus (P) from sewage and wastewater to reduce the total P load in surface water bodies, such as lakes and reservoirs [1]. At present, there are strict global restrictions on the concentration of P in discharged sewage, and the Comprehensive Sewage Discharge Standard of China (GB 8978–2002) requires that the mass concentration of phosphate (in terms of P) should be ≤0.5 mg/L [2]. In nature, P can be categorised as organic or inorganic, according to its chemical nature. Most organic P is produced in chemical plants, and although it is highly toxic, it cannot be directly utilised by organisms [3]. Inorganic P is the most dominant form of P in aquifers because almost all P exists in its pentavalent form, which becomes orthophosphate when dissolved in the aquifer. Orthophosphate, including PO_4^{3-}, HPO_4^{2-}, and $H_2PO_4^-$, is the only form of P that can be assimilated by autotrophic organisms and microorganisms in water; therefore, it is an important research target [4].

Common wastewater P removal technologies include: biological, chemical precipitation, membrane, electrochemical, and adsorption [5]. Adsorption is widely accepted as a cost-effective means of deep P removal because of its simplicity of operation, effective removal of P at low concentrations, and potential for the recovery of non-renewable P resources [6]. Adsorption is primarily used to remove orthophosphates from wastewater. Currently, metals such as iron, aluminium, calcium, magnesium, lanthanum (La), and zirconium are widely used for phosphate removal from water [7]. First, La ranks 28th in abundance in the Earth's crust, higher than common metals, such as lead and cobalt [8]. Therefore, La is not only commercially readily available and relatively inexpensive but also effectively removes low levels of P from water. This capability surpasses what traditional adsorbents like iron and aluminium can achieve. Secondly, the solubility product constant of the $LaPO_4$ precipitate generated by La ions and phosphate is extremely small, ranging from $10^{-24.7}$ to $10^{-25.7}$, making it the most insoluble of the known phosphate compounds [9]. Therefore, La-based materials offer significant advantages in terms of their P removal performance. Again, La has low-to-medium toxicity and is therefore biologically safe. It has been reported that the bioavailability of La in animals is less than 0.7‰, and the limiting utilisation rate in the human body is only 1.27‰ ± 0.8‰. Even when used orally, the vast majority of La compounds are excreted in faeces and do not accumulate in organs, such as the kidneys or bone structures [10]. In addition, La carbonate chewable tablets (fosrenol), which can effec-

* Corresponding author.
E-mail address: guangzhihu@ynu.edu.cn (G. Hu).
[1] These authors contributed equally to this work.

https://doi.org/10.1016/j.cclet.2024.110398
1001-8417/

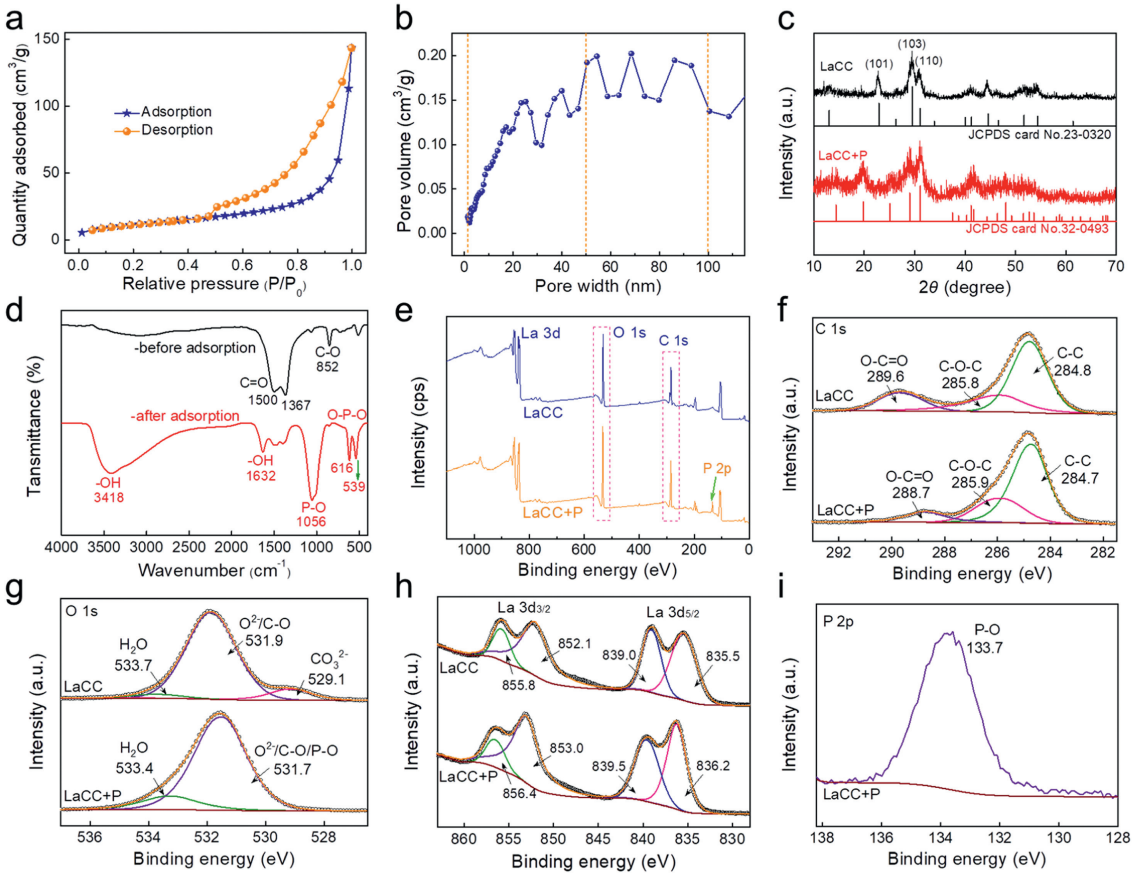

Fig. 1. (a) N_2 adsorption-desorption curves and (b) pore size distribution of LaCC. (c) XRD, (d) FTIR, and (e-i) XPS spectra of LaCC and LaCC + P.

tively reduce the P concentration in the human blood, have been successfully developed and applied in the clinical treatment of hyperphosphatemia in patients with chronic renal failure [11]. In conclusion, lanthanide-based adsorbents are safe for removing excess P from aqueous solutions.

Since there is a strong binding capacity between La ions and phosphate, it can be assumed that the La-doped adsorbent can effectively adsorb P in solution. On the other hand, the organic ligands in polymers are shed during pyrolysis thereby creating a large number of pore structures. Therefore, if the polymer is used as a carbon skeleton template, it can be assumed that the pore structure of the adsorbent will increase after pyrolysis, which will increase the diffusion rate of P on the adsorbent. In this study, adsorbent (LaCC) with honeycomb structure was prepared by vacuum freeze-drying and pyrolysis technique. The technique is easy to operate and the product is highly crystalline. The main functional component of LaCC is La carbonate oxide (La_2CO_5). Meanwhile, this study reported for the first time that lanthanum carbonate compounds were prepared by this method and used for adsorption to remove excess P from water. The influencing factors, reaction processes, and adsorption removal mechanisms of LaCC for P removal from aqueous solutions were explored. Through the above research, the P removal reaction system of the La-based carbonate adsorbent was finally established, to maximally reduce the P load into the surface water environment and provide a theoretical basis and technical support for the deep treatment of low-concentration P-containing tailwater, such as secondary effluent.

Fig. 1a shows the N_2 adsorption-desorption isothermal curve of the LaCC adsorbent, which conforms to the characteristics of the type IV curve specified by IUPAC with H3-type hysteresis loops, indicating that the synthesised adsorbent contains slit pores formed by the accumulation of banded particles [12]. The pore size distribution diagram of LaCC (Fig. 1b) shows that it has both mesoporous and macroporous multilevel structures. The phase composition of the adsorbent LaCC was analysed by X-ray diffraction (XRD) technique, and the results are shown in Fig. 1c. The positions of the corresponding diffraction peaks of the LaCC were in good agreement with the XRD standard diffraction pattern of La_2CO_5 (JCPDS card No. 23–0320), indicating that La_2CO_5 was synthesised *via* freeze-drying and pyrolysis. The functional groups contained in the adsorbent were identified by Fourier transform infrared spectrometer (FTIR) (Fig. 1d). The strong absorption bands at 1500 and 1367 cm^{-1} correspond to the asymmetric stretching vibrational peaks of C=O in CO_3^{2-} [13], and the bending vibrational peaks of CO_3^{2-} appear at 852 cm^{-1} [14]. The X-ray photoelectron spectroscopy (XPS) of LaCC before and after adsorption of P are shown in Fig. 1e. The characteristic peaks of P 2p appeared after adsorption of P. Figs. 1f-i show the XPS high-resolution maps of C, O, La, and P, respectively.

Fig. S2 (Supporting information) shows the microscopic morphology of the adsorbent. PEG provides the organic carbon skeleton structure, and the addition of La does not change the morphology of the adsorbent. The elements C, O, and La are uniformly distributed in the reticulated structure of the LaCC, indicating that La_2CO_5 is uniformly encapsulated in the organic skeleton structure provided by PEG pyrolysis. Figs. 2a and b are the transmission electron microscope (TEM) and high-resolution transmission electron microscope (HR-TEM) image of LaCC, respectively. The lattice spacing maps (Fig. 2c) of La_2CO_5 were derived from the conversion of Fig. 2a by the "Digital Micrograph" software. The spacing of Fig. 2c ①-③ is 1.950, 0.903, and 0.574 nm, representing 5, 3, and 2 lattices, respectively. Thus the spacing between neighbouring lattices

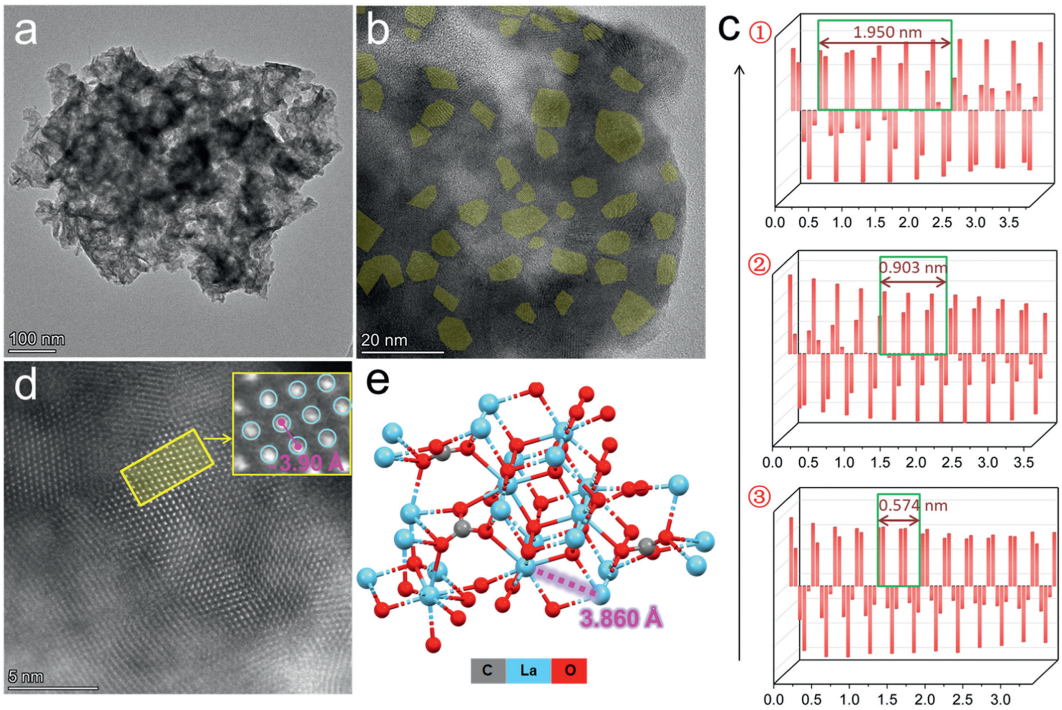

Fig. 2. (a) TEM image of LaCC. (b) HR-TEM image of LaCC. (c) Lattice spacing of La_2CO_5. (d) HAADF images of LaCC. (e) Crystal lattice model of La_2CO_5.

is 0.390, 0.301, and 0.287 nm, respectively. The lattice spacings of the 101, 103, and 110 crystal surface showed in the XRD standard card (JCPDS card No. 23–0320) of La_2CO_5 are 0.388, 0.302, and 0.287 nm, respectively, which corresponds essentially to the values of lattice spacings obtained from Fig. 2c. In the high-legged annular dark field image (HAADF) mode, the atom-sized bright spots in the lattice stripes in Fig. 2d should be La atoms, and the distance between adjacent bright spots on the lattice line was approximately 3.90 Å and this result aligns with the La-La distance within the crystal cell of La_2CO_5 (Fig. 2e, 3.86 Å). These results above further verify that the crystal structure on LaCC is La_2CO_5.

When the solution's pH changes, there are differences in the form of P and surface properties of the adsorbent, which may directly affect the binding between the adsorbent and P. The pK_a values of phosphoric acid in aqueous solutions are 2.1, 7.2, and 12.3 [15]. When the pH of the solution is <2.1, it is mainly in the form of H_3PO_4 molecules, which are not subject to electrostatic attraction; when the pH is in the range of 2.1–7.2, $H_2PO_4^-$ in the form of divalent mainly exists, and at this time, the LaCC's surface becomes positively charged due to protonation. This can produce electrostatic attraction effect with the negative ions of phosphate and thus promote the phosphate removal (Fig. 3a) [16]. At pH >7.2, HPO_4^{2-} gradually replaced $H_2PO_4^-$ as the most dominant form. At this time, the amount of positive charge carried on the LaCC surface gradually decreased, resulting in weakening of the electrostatic attraction and inhibition of phosphoric acid removal by adsorption. As the solution's pH continues to rise, surpassing the isoelectric point of LaCC at 10.1 (pH_{pzc}) (Fig. 3b), the surface of the LaCC starts to be negatively charged by deprotonation, which can produce electrostatic repulsive action with the equally negatively charged phosphate and inhibit the adsorption removal of P [17]. In contrast, OH^- increased with increasing pH, thereby inhibiting the adsorption of phosphate by the LaCC.

The leaching of La of the adsorbent LaCC was examined under different pH conditions. When the pH value was below 3, the La concentration in the solution was higher than 29.3 mg/L, indicating a higher risk of La leakage in the LaCC under strongly acidic conditions. When the pH rises, less La was released. When the pH exceeds 5, the leaching of La is minimal, measuring only 126 μg/L. This concentration falls below the maximum allowable limit of 150 μg/L for total La in freshwater according to Dutch regulations [18]. Given that the typical pH range for natural or domestic wastewater lies between 6.5 and 8.5 [14], there is no need to overly concerned about La leakage.

Figs. 3c and d show the fitted model plots for kinetics and isotherms, respectively. Table S2 (Supporting information) shows that the Langmuir model exhibits higher correlation coefficients compared to the Freundlich model. This suggests that the Langmuir model provides a better fit, implying a uniform monolayer adsorption process for P by LaCC. This conclusion is similar to those of related studies on other lanthanide-based adsorbents [19].

Table S3 (Supporting information) shows that the correlation coefficient (R^2) for the *pseudo*-second-order model was notably high. Furthermore, the maximum adsorption capacities predicted by the *pseudo*-second-order model (97.9, 108.4, and 112.5 mg P/g) closely matched the experimental values (99.9, 110.9, and 116.7 mg P/g) across various P concentrations. Thus, it can be hypothesised that the process of phosphate adsorption by LaCC is mainly chemisorption, which produces strong chemical bonds through ligand exchange [20].

Australia's Commonwealth Scientific and Industrial Research Organisation (CSIRO) has developed La-modified bentonite, which finds extensive use in real-world water treatment projects [21]. Unfortunately, the adsorbent has a limited adsorption capacity, approximately 10 mg P/g. Therefore, it is essential to improve the adsorption capacity of P adsorbents. The adsorption capacities of the LaCC and previously reported P adsorbents of the same type were compared (Table S4 in Supporting information). The P adsorption capacity of LaCC has a clear advantage, indicating that it has great potential for practical applications. The fixed-bed experiment was conducted to evaluate the removal efficiency of LaCC on low concentration P in continuous flow, and the device diagram was shown in Fig. 4a. Fig. 4b showed that 1020 BV of P-containing solution was effectively treated in the initial fixed-bed experiment.

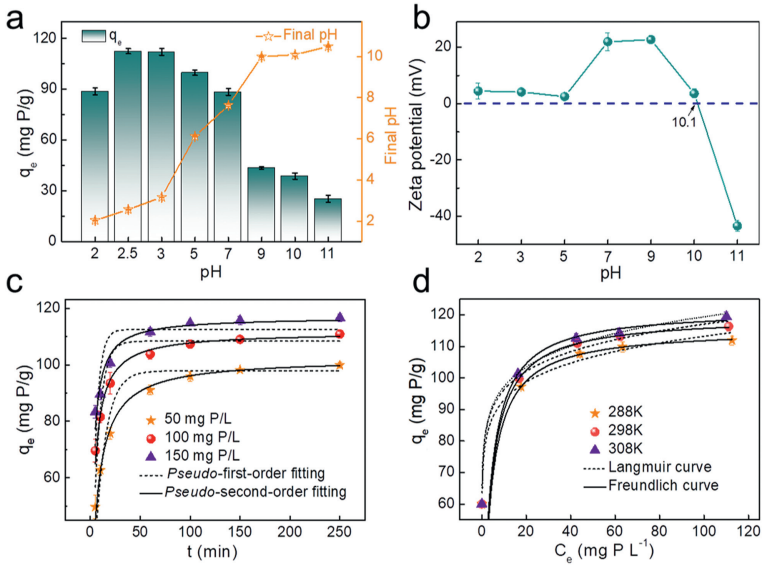

Fig. 3. (a) Effect of pH on the adsorption of P by LaCC (*T*: 298 K; dosage of LaCC: 1/3 g/L; C_0: 50 mg P/L; adsorption time: 5 h). (b) Zeta potential of LaCC. (c) Adsorption kinetics of P-adsorption on LaCC. (d) Adsorption isotherms of P-adsorption on LaCC (C_0: from 20 mg P/L to 150 mg P/L; reaction time: 5 h). (c, d) *T*: 298 K; dosage: 1/3 g/L).

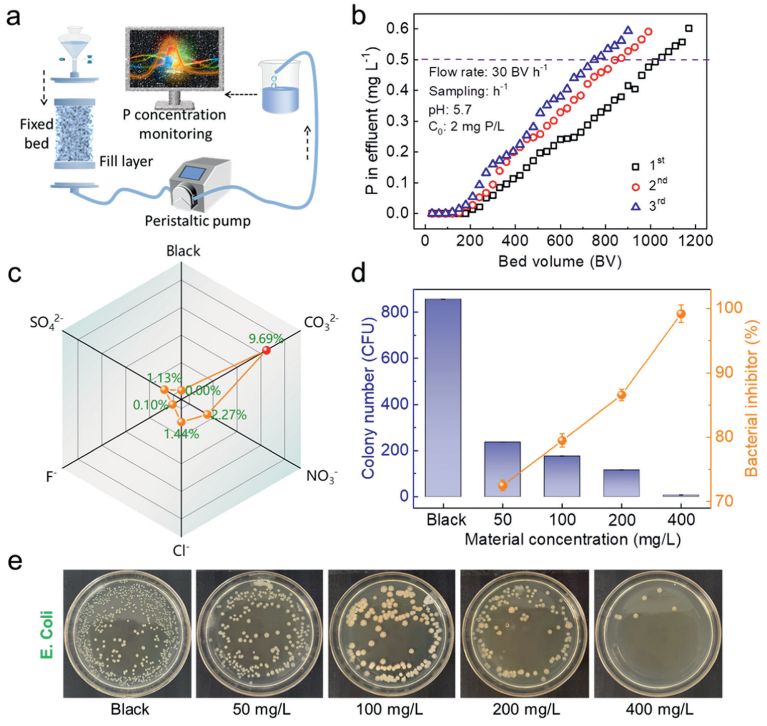

Fig. 4. (a) Fixed bed device diagram. (b) Breakthrough curves of LaCC. (c) Effects of coexisting ions on the adsorption of P by LaCC. (d, e) Inhibition of *E. coli* at different concentrations of LaCC.

Remarkably, just 1 g of LaCC could treat approximately 60 L of P-containing wastewater. Following breakthrough, the fixed bed filler was desorbed in place using NaOH (1 mol/L). In the next two cycle experiments, 840 and 750 BV of water were effectively treated, which were 82.4% and 73.5% of the initial treated water volume, respectively, verifying that the LaCC adsorbent has a higher potential for the application of P adsorption in real wastewater.

Common anions in the water column, such as Cl^-, F^-, SO_4^{2-}, CO_3^{2-}, and NO_3^-, were selected to explore the anti-interference ability of LaCC. Fig. 4c shows that Cl^-, F^-, SO_4^{2-}, and NO_3^- hardly affected the adsorption of P by LaCC even when their concentration (200 mg/L) was much higher than that of P. However, the inhibition of CO_3^{2-} was more pronounced and the inhibition rate was 9.69%. This may be because the addition of CO_3^{2-} increases the pH of the solution, which is unfavourable for phosphate removal [22]. However, $La_2(CO_3)_3$ has a lower solubility than $LaPO_4$, which makes it easier to generate [23]. However, even in this case, LaCC adsorption still reach 91.8 mg P/g, suggesting that LaCC are highly selective for phosphate ions and have great potential for practical applications.

If an adsorbent can achieve both P removal and sterilisation in wastewater, its application range will increase. Figs. 4d and e show that the growth of *E. coli* added to the LaCC was inhibited when the inoculum concentration of the strain was kept the same, and the inhibition effect was gradually obvious with increasing LaCC

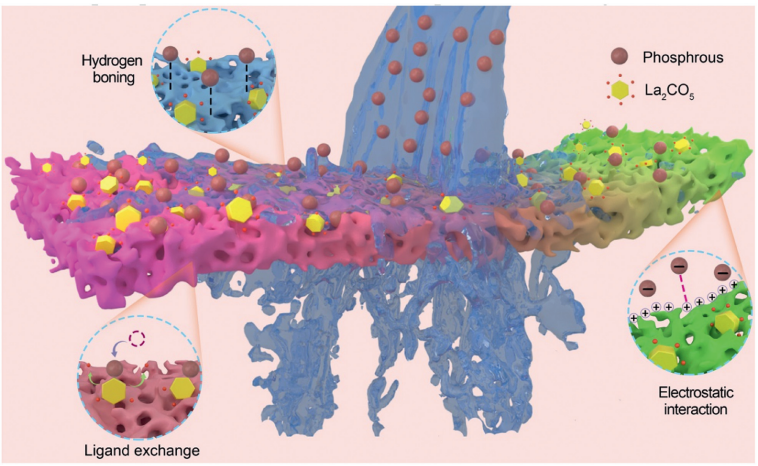

Fig. 5. Adsorption mechanism of P by LaCC.

dosing. Based on colony counts, the inhibition rates for *E. coli* were 72.5%, 79.5%, 86.6%, and 99.2% at dosages of 50, 100, 200, and 400 mg/L, respectively. Some metal ions such as silver, copper, zinc, iron [24], and La [25] exhibit antibacterial properties. When the La ions reached 100 μg/L, it killed ~39% of *E. coli* in only one minute [26]. The pH of the medium was around 7.4, and under these conditions, when LaCC was dosed at 50, 100, 200, and 400 mg/L, the amount of La leached from the solution was 32, 61, 108, and 173 μg/L, respectively, thus inhibited the growth and reproduction of *E. coli*. In addition, the adsorbent LaCC adsorbents may inhibit the uptake of nutrients such as carbon, nitrogen, and P by bacteria, resulting in their inability to grow properly [27].

Fig. 5 shows the reaction mechanisms involved in the adsorption of P by the LaCC, including electrostatic attraction, hydrogen bonding, and ligand exchange interactions [28]. During the increase in solution pH from acidic to the isoelectric point of LaCC, positively charged adsorbent surfaces rapidly attract P through electrostatic forces, forming stable inner complexes *via* ligand exchange (Eqs. 1–3) [13,29]. At neutral pH, phosphate anions ($H_2PO_4^-$ and HPO_4^{2-}) can interact with the adsorbent as both hydrogen-bond acceptors and donors [30]. Although the electrostatic gravitational effect continued to weaken with increasing solution pH, the dominant ligand exchange mechanism was sufficient to counteract this negative effect. When the pH of the solution continued to increase, OH^- competed with phosphate for the CO_3^{2-} sites. Therefore, the desorption of P can be achieved by placing the LaCC into a strongly alkaline solution.

The adsorption mechanism was further elucidated by comparing the LaCC sample characterisation results before and after P adsorption. The positions of the diffraction peaks of the LaCC after the adsorption of P were in good agreement with the XRD standard diffraction pattern of $LaPO_4$ (JCPDS Card No. 32–0493), indicating that the phosphates bound to La in the LaCC. Fig. 1d shows that the peaks located at 1632 and 1056 cm^{-1} correspond to the -OH stretching vibrational peak in $H_2PO_4^-$ and the symmetric stretching vibrational peak of P-O, respectively [13]; and the peaks located at 616 and 539 cm^{-1} correspond to the phosphate groups' vibrational peaks of *v*4 [31]. In addition, the intensities of all the CO_3^{2-} peaks of the LaCC after the adsorption of P decreased significantly, indicating that CO_3^{2-} plays a crucial role in the adsorption process.

The XPS total spectra showed that a P 2p signal peak was detected in the LaCC after the adsorption of P (Fig. 1e). The fitting results of the C 1s signal peak show that the position of the O–C=O bond belonging to CO_3^{2-} shifts from 289.6 eV to 288.7 eV, and the content decreases from 18.1% to 10.8% (Fig. 1f). In addition, no characteristic peaks belonging to CO_3^{2-} were fitted on LaCC after adsorption of P (Fig. 1g), indicating that CO_3^{2-} participates in the reaction and ligand exchange is the main adsorption mechanism. The double split peaks at 835.5 and 852.1 eV correspond to the La $3d_{5/2}$ and La $3d_{3/2}$ eigenpeaks (Fig. 1h), these peaks exhibit a spin-orbit splitting energy of 16.6 eV After P were adsorbed, the La 3d characteristic peak moved to a higher binding energy of approximately 0.7 eV, suggesting a possible electron transfer between phosphate and LaCC to form complexes containing La–O–P chemical bonds [32].

$$La_2CO_5 + 2H_2PO_4^- \rightarrow La_2O_2(H_2PO_4)_2 + CO_3^{2-} \quad (1)$$

$$La_2CO_5 + HPO_4^{2-} \rightarrow La_2O_2(HPO_4) + CO_3^{2-} \quad (2)$$

$$La_2CO_5 + PO_4^{3-} \rightarrow La_2O_2(PO_4)^- + CO_3^{2-} \quad (3)$$

This study reports for the first time the growth of La_2CO_5 on carbon skeletons using vacuum freeze-drying and carbonisation techniques and its use for the removal of excess P from wastewater. PEG has a carbon skeleton that allows La_2CO_5 to be uniformly distributed inside the adsorbent. The carbonation process generates gases and gas spillage creates a rich pore structure, and this structure enhances the active sites. The LaCC exhibited a remarkably high P adsorption capacity, reaching 119.5 mg P/g. This value significantly surpassed that of a similar type of P adsorbent. The dynamic experiment showed that LaCC has an excellent P removal effect, which is attributed to its rapid adsorption kinetics. In addition, the LaCC adsorbent inhibited the growth of *E. coli* during P removal, making this multifunctional adsorbent more promising for practical applications. This study confirms the safety of the LaCC adsorbent and its practical viability for treating sewage and wastewater. It establishes a theoretical foundation and offers technical backing for the efficient removal of P from these environmental sources.

Declaration of competing interest

The authors declare that they have no known competing financial interests or personal relationships that could have appeared to influence the work reported in this paper.

CRediT authorship contribution statement

Xiuxiu Jia: Writing – original draft, Investigation, Data curation, Conceptualization. **Tao Yin:** Visualization, Investigation. **Nianpeng**

Li: Resources, Methodology. **Hua Zhang:** Methodology, Formal analysis. **Anxian Shi:** Resources, Formal analysis. **Abdukader Abdukayum:** Methodology, Formal analysis. **Sanshuang Gao:** Investigation, Formal analysis. **Guangzhi Hu:** Writing – review & editing, Validation, Supervision, Project administration, Funding acquisition.

Acknowledgments

This work was financially supported by Science and Technology Talent and Platform Program of Yunnan Provincial Science and Technology Department (No. 202305AM070001), Zhaotong Phoenix Plan (2021), Double-First Class University Plan (No. C176220100042), and the Postgraduate Research and Innovation Foundation of Yunnan University (No. KC-23234662). The authors thank Advanced Analysis and Measurement Center of Yunnan University for the sample testing service.

Supplementary materials

Supplementary material associated with this article can be found, in the online version, at doi:10.1016/j.cclet.2024.110398.

References

[1] Q. He, X. Li, Y. Ren, Biochar 4 (2022) 25.
[2] W. Yang, X. Shi, H. Dong, et al., Chem. Eng. J. 405 (2021) 126649.
[3] W. Feng, T. Wang, Y. Zhu, et al., Carbon Res. 2 (2023) 12.
[4] P. Roots, F. Sabba, A.F. Rosenthal, et al., Environ. Sci. Wat. Res. 6 (2020) 566–580.
[5] N. Sornhiran, S. Aramrak, N. Prakongkep, W. Wisawapipat, Biochar 4 (2022) 2.
[6] H. Chen, Y. Gao, J. Li, et al., Carbon Res. 1 (2022) 4.
[7] R. Li, Q. Zhu, S. Lu, Appl. Surf. Sci. 640 (2023) 158459.
[8] J.V. Nolan, J.W. Brakebill, R.B. Alexander, G.E. Schwarz, Geological Survey Open–File Report 02-40, U.S, Geological Survey, Reston, VA, 2002.
[9] B. Wu, L. Fang, J.D. Fortner, X. Guan, I.M.C. Lo, Water Res. 126 (2017) 179–188.
[10] M. Pennick, K. Dennis, S.J.P. Damment, J. Clin. Pharmacol. 46 (2006) 738–746.
[11] S.J.P. Damment, M. Pennick, Clin. Pharmacokinet. 47 (2008) 553–563.
[12] M. Thommes, K. Kaneko, A.V. Neimark, et al., Pure. Appl. Chem. 87 (2015) 1051–1069.
[13] Y. Huang, Y. He, H. Zhang, et al., J. Environ. Chem. Eng. 10 (2022) 107476.
[14] S. Shan, W. Wang, D. Liu, et al., J. Hazard. Mater. 397 (2020) 122597.
[15] M. Du, Y. Zhang, Z. Wang, et al., Chem. Eng. J. 442 (2022) 136147.
[16] Q. He, H. Zhao, Z. Teng, et al., Sep. Purif. Technol. 314 (2023) 123529.
[17] Y. Zhang, Y.F. Xiao, G.S. Xu, et al., J. Environ. Chem. Eng. 11 (2023) 109995.
[18] X. Jia, X. Zhao, Y. Zhou, et al., Biochar 5 (2023) 16.
[19] W. Xu, W. Zheng, F. Wang, et al., Chem. Eng. J. 403 (2021) 126349.
[20] P. Wang, L. Li, Y. Tian, et al., Sci. Total. Environ. 809 (2022) 152124.
[21] X. Jia, T. Yin, Y. Wang, et al., Biochar 5 (2023) 84.
[22] S.Y. Lee, J.W. Choi, K.G. Song, et al., Compos. Part. B: Eng. 176 (2019) 107209.
[23] J. Qu, M.S. Akindolie, Y. Feng, et al., Chem. Eng. J. 394 (2020) 124915.
[24] Q. Ye, W. Chen, H. Huang, et al., Appl. Microbiol. Biot. 104 (2020) 5213–5227.
[25] J. He, W. Wang, F. Sun, et al., ACS Nano 9 (2015) 9292–9302.
[26] J. He, W. Wang, W. Shi, F. Cui, RSC Adv. 6 (2016) 99353–99360.
[27] X. Zhang, W. Wang, W. Shi, et al., J. Mater. Chem. A 4 (2016) 12799–12806.
[28] S.B. Liu, X.F. Tan, Y.G. Liu, et al., RSC Adv. 6 (2016) 5871–5880.
[29] S. Ahmed, N.M. Ashiq, D. Li, et al., Recent Pat. Nanotech. 13 (2019) 3–16.
[30] B. Wu, J. Wan, Y. Zhang, B. Pan, I.M.C. Lo, Environ. Sci. Technol. 54 (2020) 50–66.
[31] X. Jia, X. Zhao, Z. Bi, et al., Sep. Purif. Technol. 306 (2023) 122713.
[32] Y. Gu, D. Xie, Y. Ma, et al., ACS Appl. Mater. Interfaces 9 (2017) 32151–32160.